European Radiology (2018) 28:3770–3778
https://doi.org/10.1007/s00330-018-5388-0

UROGENITAL

T2-weighted balanced steady-state free procession MRI evaluated for diagnosing placental adhesion disorder in late pregnancy

Ang Yang[1] · Xue Hong Xiao[1] · Zhi Long Wang[1] · Ze Yan Wang[1] · Ke Yi Wang[1]

Received: 24 November 2017 / Revised: 19 January 2018 / Accepted: 16 February 2018 / Published online: 12 April 2018

Abstract

Objective This study evaluated the imaging characteristics and accuracy of T2-weighted (T2W) balanced steady-state free procession (b-SSFP) magnetic resonance imaging, relative to b-SSFP or single-shot fast spin echo (SSFSE), for the diagnosis of placental adhesion disorder (PAD). Methods: Fifty-one pregnant patients suspected of PAD were examined with T2W b-SSFP, b-SSFP and SSFSE. The image types were independently analysed for signs of PAD: abnormal placental bulge (APB), dark intraplacental bands (DIB), placental heterogeneity (PH) and placental protrusion into adjacent structures (PPAS). The sequences were compared for muscle-to-placenta signal ratio, signs of PAD and area under the receiver operating characteristic curve (AUC) for diagnostic accuracy of PAD.

Results PAD was confirmed in 34 women. The muscle-to-placenta signal ratio was highest in the T2W b-SSFP. The diagnostic rates of APB in T2W b-SSFP were comparable to that of b-SSFP, but were significantly higher than that of SSFSE. The rates of PH in SSFE were comparable to that of b-SSFP, but both were significantly lower than that of T2W b-SSFP. The rates of DIB were significantly higher in T2W b-SSFP images compared with SSFSE. Rates of PPAS were comparable among three sequences. The AUCs of the T2W b-SSFP, b-SSFP and SSFSE were 0.966, 0.890 and 0.823, respectively.

Conclusion T2W b-SSFP has high diagnostic accuracy for PAD relative to SSFSE or b-SSFP, which may be due to its high SNR, T2-weighting and lack of blur.

Key Points

- *Signal myometrium-to-placenta ratio was highest in the T2W b-SSFP images.*
- *Diagnostic rate of APB in T2W b-SSFP was highest.*
- *Diagnostic rate of DIB was higher in T2W b-SSFP than in SSFSE.*
- *Diagnostic rate of PH in T2W b-SSFP was highest.*
- *Maximum AUC for diagnostic accuracy of PAD was in T2W b-SSFP.*

Keywords Placenta accreta · Magnetic resonance imaging · Pregnancy · Diagnosis · ROC curve

Abbreviations

APB	Abnormal placental bulge
AUC	Receiver operating characteristic curve
b-SSFP	Balanced steady-state free procession
DIB	Dark intraplacental bands
FFE	Fast field echo
M2D	Multiple (sequential) 2D slices
NSA	Number of signals averaged
PAD	Placental adhesion disorder
PH	Placental heterogeneity
PPAS	Placental protrusion into adjacent structures
ROI	Region of interest
SE	Spin echo
SNR	Signal-to-noise
SPIR	Spectral presaturation inversion recovery
SSFSE	Single-shot fast spin echo
T2W	T2-weighted
TFE	Turbo field echo

✉ Ang Yang
yang19781230@gmail.com

[1] MR department of Affiliated Zhongshan City Hospital of Sun Yat-sen University, Sun Wendong Road No. 2, Zhongshan City, Guangdong Province, China

Introduction

Placental adhesion disorder (PAD) is characterized by the extension of chorionic villi or trophoblastic tissue beyond the decidua to reach the underlying myometrium or serosa of the uterus. According to the depth of invasion, PAD is classified as placenta accreta vera, increta or percreta: villi attached to the superficial myometrium only; partially invading the myometrium; or invading up to or beyond the uterine serosa, respectively [1]. While still considered rare, PAD is positively associated with maternal age and repeat caesarean deliveries [2–4], and its incidence has increased 10-fold in the past 50 years [5]. Indeed, prior caesarean section and placenta praevia are the most important risk factors for PAD [4].

PAD can result in massive post-partum haemorrhage that can require multiple blood transfusions and emergency hysterectomy, with associated maternal morbidity and mortality [6]. To minimise perinatal complications, accurate prenatal imaging that identifies the type and extent of abnormal placentation is important during delivery planning.

Ultrasound has been considered sufficient for the diagnosis of PAD, with supplementary magnetic resonance imaging (MRI) in cases with equivocal sonographic findings or posterior placenta accreta [7]. MRI is superior for characterizing extra-uterine placental invasion [8]. In practice, MRI sequences routinely used for diagnosis include multiplanar T2-weighted (T2W) single-shot fast spin echo (SSFSE/HASTE/SSHTSE depending on the vendor); balanced steady-state free procession (b-SSFP) (B-TFE/True FISP/FIASTA depending on the vendor); T1WI, in-phase and opposed-phase; and non-contrast fat-saturated 3D T1W gradient echo sequences [1, 5, 8–11]. The T2W b-SSFP uses a 180° of flip angle to make the b-SSFP have T2-weighted features. While preserving the advantages of b-SSFP's high signal-to-noise (SNR) ratio, short imaging time and lack of blur, T2W b-SSFP also provides greater tissue contrast.

We hypothesised that T2W b-SSFP was superior to SSFSE or b-SSFP in diagnosing PAD. In this study, T2W b-SSFP, b-SSFP and SSFSE were used in diagnosing PAD, and imaging characteristics and diagnostic accuracy of three sequences were compared; the features of T2W b-SSFP were also discussed.

Methods

Subjects

The local institutional ethics review board approved this study and informed consent was obtained. This prospective study population comprised 51 pregnant women (aged 32.6 ± 4.7 years) who had been consecutively investigated using prenatal MRI between August 2014 and June 2017, after obstetric referral for suspected placental invasion based on standard pregnancy US and clinical histories and symptoms. The patients who could not complete or were not suitable for MRI examination, and those who not had a caesarean section in our institution were excluded. The gestational age of all the patients was greater than 28 weeks (35.4 ± 3.6 weeks). Of the 51 patients, 40 had placenta praevia; and 42, 9 and 9 patients had histories of caesarean delivery, curettage and myomectomy, respectively; 15 patients had a history of vaginal bleeding.

MRI protocols

All subjects underwent MRI with a 1.5-T MR scanner (Intera Systems, Philips, Netherlands) equipped with a SENSE cardiac coil. The MRI examinations usually did not exceed 15 min. The MRI protocols included T2W SSFSE, b-SSFP and T2W b-SSFP in the axial, sagittal and coronal planes (Table 1). The patients were free to breathe during all sequences (without respiratory triggering).

In SSFSE, fat suppression was obtained with frequency-selective fat saturation to reduce chemical shift artefacts [12]. The flip angle of the refocusing pulses was set to 130° to lower specific radiofrequency absorption with only a slight sacrifice of SNR ratio [13].

In T2W b-SSFP and b-SSFP, the volume shim (which included as much placenta as possible) was used to reduce field inhomogeneities and artefacts at tissue interfaces. Echo time (TE)/repetition time (TR) was set to 1/2 to obtain the best SNR. TR was set to 5 ms to obtain a balance between high SNR and low banding artefacts. The scanning times of T2W b-SSFP were about 1 s per slice, and mean duration was about 40 s varying with the number of slices acquired.

Image analysis

All data were imported into clinical workstations (ONIS 2.0 free version, Tokyo, Japan, http://www.onis-viewer.com/) for data analysis. A radiologist with 5 years of experience in obstetrics and gynaecologic MRI measured the signal ratio of myometrium-to-placenta in the three MRI sequences (Fig. 1).

Two obstetric and gynaecologic radiologists, with respectively 8 and 10 years of experience in MRI, participated in reading the images for diagnosis of PAD. They were informed of the primary aim of the study but were blinded to patient identity and the results of other imaging studies, as well as surgical and histologic results. Before the reading sessions, both observers underwent a training session regarding the four signs of PAD, namely abnormal placental bulge (APB), dark intraplacental bands (DIB), placental heterogeneity (PH) and placental protrusion into adjacent structures (PPAS). These signs are described below.

An APB was observed as a disruption of the continuity of the curve on the maternal side of the placenta, which does not

Table 1 MRI examination parameters of the three MRI sequences

	SSFSE [a]	Balanced SSFP [b]	T2W b-SSFP [b]
Field of view (mm)	320–350	320–350	320–350
Voxel (mm)	1.5 × 1.5	1.5 × 1.5	1.5 × 1.5
Slice thickness (mm)	4.5	4.5	4.5
Fold over suppression	Yes	No	No
Sense	2.0	2.0	2.0
Scan mode	M2D	M2D	M2D
Technique	SE	FFE	FFE
Fast mode	FSE	TFE	TFE
Shot mode	Single shot	Single shot	Single shot
Profile order	Linear	Linear	Linear
Start-up echoes	8	Default	Default
Flip angle (°)	90	80	180
TE (ms)	90	2.5	2.5
TR (ms)	2000	5	5
Water–fat shift	Maximum	0.42–0.58	0.42–0.58
Fat suppression	SPIR	NA	NA
Shim	Default	Volume	Volume
NSA	1	1	1

M2D multiple (sequential) 2D slices, *FFE* fast field echo, *NSA* number of signals averaged, *SE* spin echo, *SPIR* spectral presaturation inversion recovery, *TFE* turbo field echo

[a] Refocusing control, 130°

[b] Contrast enhancement, balanced

include placental deformation caused by adjacent structures such as fibroids and the aorta (Fig. 2). DIB originate from the basilar plate at the maternal side of the placenta, with a length greater than 2 cm (Fig. 3) [14]. PH appears as marked heterogeneity in the placenta, but does not include DIB (Figs. 4 and 5). PPAS is defined as an extension of placental tissue beyond the uterine serosa into the parametrium, bladder or bowel, or superimposed placental protrusion into the internal cervical os (Fig. 5) [4, 15].

To minimise recall bias, the T2W b-SSFP, b-SSFP and SSFSE images were analysed in separate sessions, at least 6 weeks apart. Two radiologists read the images together and achieved a consensus after discussion. During the reading sessions, whether or not there were the signs such as APB,

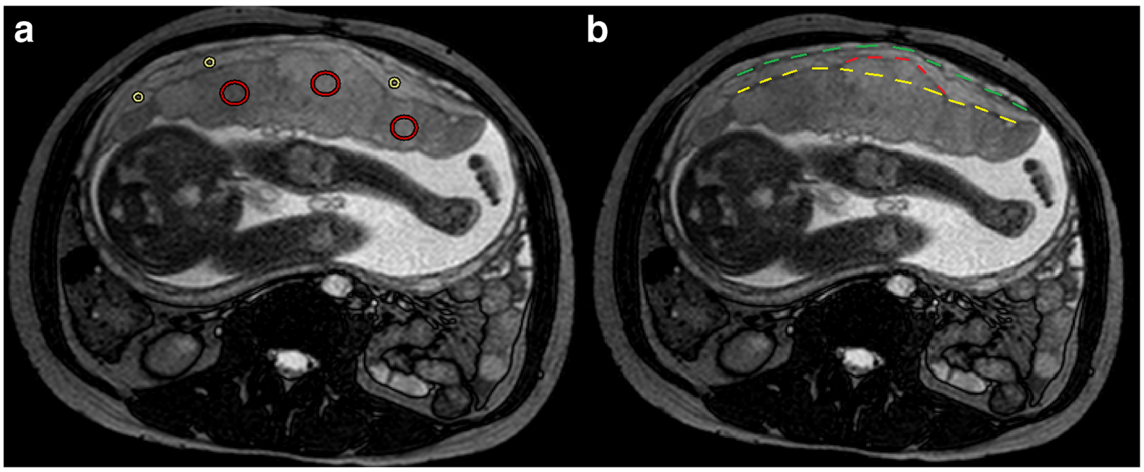

Fig. 1 Representative case of confirmed placenta increta. Signal ratio of myometrium-to-placenta and the sign of APB. **a** ROIs were selected and averaged respectively on both the placenta and myometrium, and the signal ratio of myometrium-to-placenta calculated. **b** The yellow line indicates the contour of a normal placenta, the red line shows the placental bulge and the green line represents the contour of the uterus. The prominent placenta bulge, with no obvious uterine wall bulge, led to the diagnosis of PAD

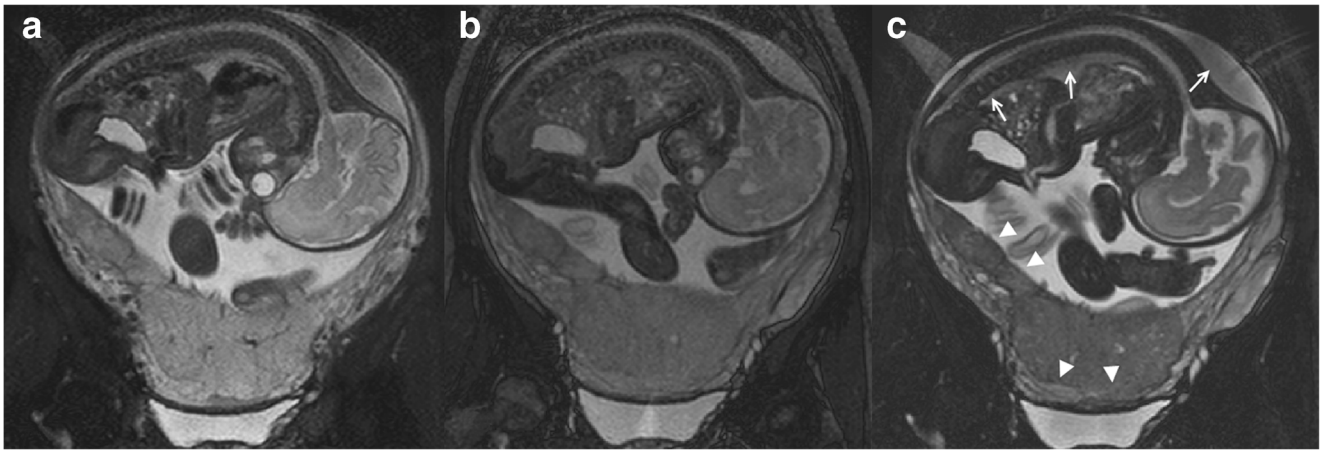

Fig. 2 Representative case of confirmed placenta increta, illustrated with an APB with different MRI sequences. **a** SSFSE; **b** same layer in b-SSFP; **c** same layer in T2W b-SSFP. Note the higher SNR (arrows) and clearer placental outline (triangles) in the T2W b-SSFP

DIB, PH and PPAS was recorded. At the end of the reading, the radiologists were asked to give a diagnostic score of PAD (1, definitely no PAD; 2, probably not PAD; 3, indeterminate; 4 probably PAD; and 5, definitely PAD). The scoring is subjective and followed as below: if there is a PPAS, then, whether or not there are other signs, scoring 5; if all signs are not present, scoring 1; 2–4 is scored on the basis of the presence of the APB, DIB or PH signs, as well as their quantity and severity.

Standard of reference

The reference standard for determining the status of the placenta consisted of intraoperative findings in all patients and the results of histopathological examinations of the removed uterus of patients who had a hysterectomy. The final diagnosis regarding the status of the placenta was based on well-established criteria [16, 17], briefly as follows. Placenta accreta vera cannot be self-stripping from the uterine wall during vaginal delivery or caesarean section. Manual removal revealed that the placenta adhered to the uterine wall but was still able to be separated. Partial absence of basal decidua was found on pathological examination. In increta, total manual removal of the placenta is impossible and resulted in massive bleeding from the implantation site after difficult manual removal; histological confirmation of villi invading the myometrium on hysterectomy specimens. Percreta was confirmed during surgery when complete invasion of the myometrium and uterine serosa, or invasion of adjacent organs, was observed.

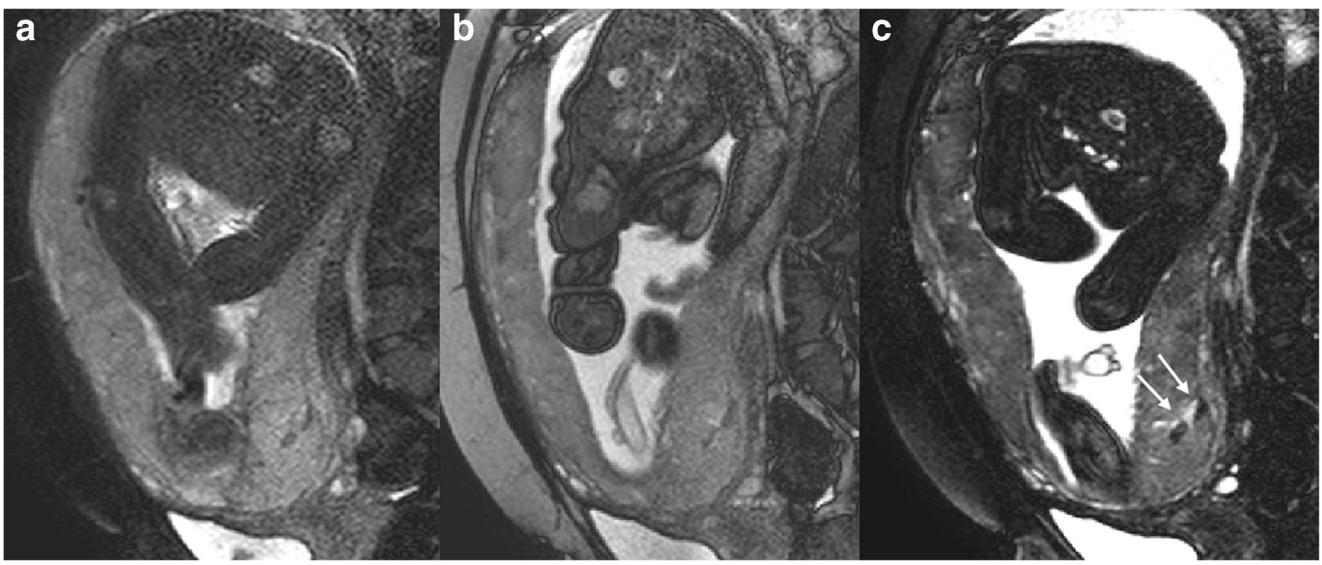

Fig. 3 Representative case of confirmed placenta accreta vera, showing DIB with different MRI sequences. **a** SSFSE; **b** same layer in b-SSFP; **c** same layer in T2W b-SSFP. Note that the low signal band is most pronounced in the T2W b-SSFP (arrow)

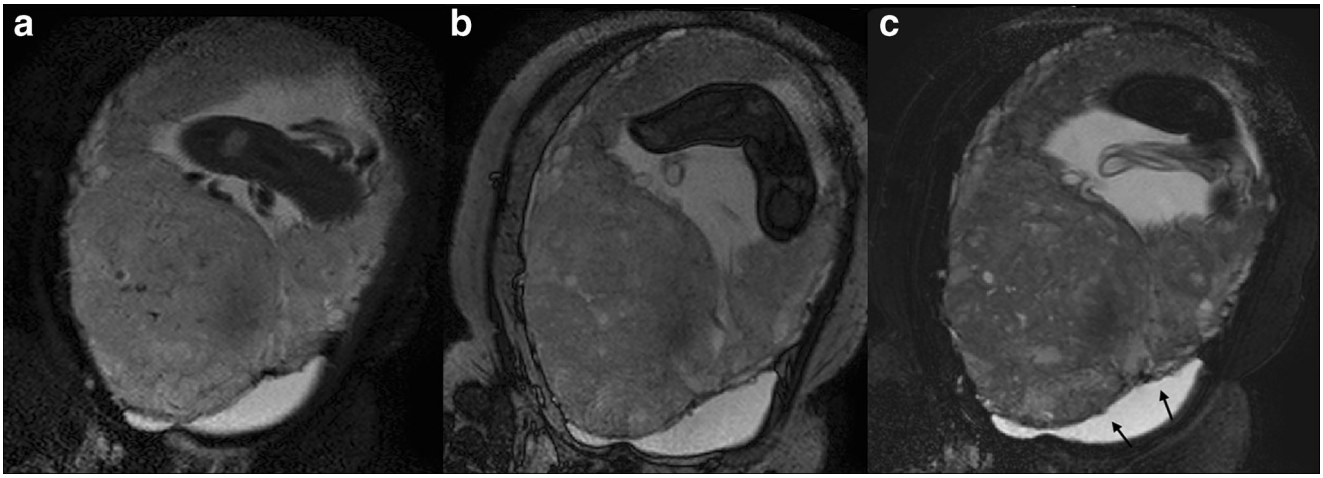

Fig. 4 Representative case of confirmed placenta percreta, with PH shown in different MRI sequences. **a** SSFSE; **b** same layer in b-SSFP; **c** same layer in T2W b-SSFP. Note the obvious heterogeneous placenta in the T2W b-SSFP, and that the placenta is blurred with the bladder wall, and the bladder has serration (arrow)

Statistical analysis

Statistical analyses were performed using SPSS (v.19.0) software, and the threshold for statistical significance was set at $p < 0.05$.

The myometrium-to-placenta signal ratios of the three MRI sequences were compared using the paired-samples *t* test. The detection of the four signs of PAD (i.e. APB, DIB, PH and PPAS) in the three MRI sequences was compared using McNemar's test.

The area under the receiver operating characteristic (ROC) curve (AUC) was used for statistical analyses of the accuracy of the three MRI sequences for diagnosis of PAD.

In T2W_bSSFP, the diagnostic sensitivity and specificity of three signs (APB, DIB and PH) for accreta vera and increta were obtained, and Youden index values were obtained by calculating sensitivity + specificity − 1.

Results

Among the 51 patients, 34 were confirmed to have PAD on the basis of surgery and pathology results (8, 19 and 7 cases of placenta accreta vera, increta and percreta, respectively); 17 were confirmed to be without PAD.

The signal myometrium-to-placenta ratio was significantly higher in the T2W b-SSFP images (1.44 ± 0.14) compared with the b-SSFP (1.23 ± 0.11; $p < 0.001$), which in turn was significantly higher than the SSFSE (1.18 ± 0.12; $p = 0.041$; Table 2).

The detection rate of APB in T2W b-SSFP (70.5%) was comparable to that of b-SSFP (60.7%; $p = 0.125$; Table 3). However, the rate of APB in either T2W b-SSFP images or b-SSFP images was significantly higher than in the SSFSE (47.0%; $p = 0.004$ and 0.039, respectively).

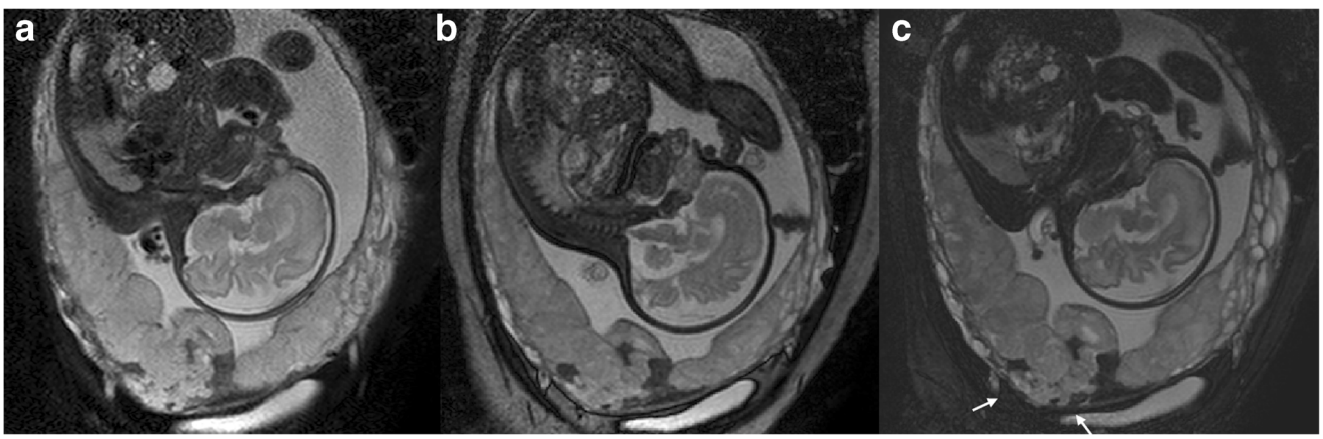

Fig. 5 Representative case of confirmed placenta percreta, with PPAS shown in different MRI sequences. **a** SSFSE; **b** the same layer in b-SSFP; **c** the same layer in T2W b-SSFP. The placenta protrudes through the wall of the uterus and several DIB were also observed

Table 2 Signal myometrium-to-placenta ratio in three MRI sequences

	Signal ratio	*p* value
T2W b-SSFP vs. b-SSFP	1.44 ± 0.14 vs. 1.23 ± 0.11	< 0.001
T2W b-SSFP vs. SSFSE	1.44 ± 0.14 vs. 1.18 ± 0.12	< 0.001
b-SSFP vs. SSFSE	1.23 ± 0.11 vs. 1.18 ± 0.12	0.041

T2W T2-weighed, *b-SSFP* balanced steady state free procession, *SSFSE* single-shot fast spin echo

The detection rate of DIB was significantly higher in T2W b-SSFP images (56.8%) compared with SSFSE (43.1%; $p = 0.039$; Table 3). The detection rate of PH in T2W b-SSFP (52.9%) was significantly higher than in b-SSFP (25.4%; $p < 0.001$) or SSFSE (23.5%; $p < 0.001$); however, b-SSFP and SSFSE were comparable. Among the three MRI sequences, the rates of PPAS were statistically similar.

For accuracy of diagnosis of PAD, the maximum AUC was found in T2W b-SSFP (0.966), followed by b-SSFP (0.890), and SSFSE (0.823), each with a *P* value less than 0.001 (Fig. 6).

In T2W_bSSFP, the highest diagnostic sensitivity was 92.6% for APB and highest specificity was 88.2% for DIB. The highest Youden index was 69.1% for APB, followed by 66% for DIB, and 43.2% for PH (Table 4).

Discussion

To our best knowledge, it is the first report to apply the T2W b-SSFP in diagnosing PAD. Three fast imaging sequences for examining PAD were compared in this study: T2W b-SSFP, b-SSFP and SSFSE. T2W b-SSFP had the highest myometrium-to-placenta signal ratios. T2W b-SSFP also had a higher rate of diagnosis of APB and DIB compared with SSFSE. Of the three MRI sequences, T2W b-SSFP showed the maximum AUC for diagnostic accuracy of PAD. All the above confirms the hypothesis that T2W b-SSFP was superior to SSFSE or b-SSFP in diagnosing PAD.

Table 3 Signs of PAD in three MRI sequences

		Detection rate	*p* value
APB	T2W b-SSFP vs. b-SSFP	70.5% vs. 60.7%	0.125
	T2W b-SSFP vs. SSFSE	70.5% vs. 47.0%	0.004
	b-SSFP vs. SSFSE	60.7% vs. 47.0%	0.039
DIB	T2W b-SSFP vs. b-SSFP	56.8% vs. 50.9%	0.250
	T2W b-SSFP vs. SSFSE	56.8% vs. 43.1%	0.039
	b-SSFP vs. SSFSE	50.9% vs. 43.1%	0.219
PH	T2W b-SSFP vs. b-SSFP	52.9% vs. 25.4%	< 0.001
	T2W b-SSFP vs. SSFSE	52.9% vs. 23.5%	< 0.001
	b-SSFP vs. SSFSE	25.4% vs. 23.5%	1.000
PPAS	T2W b-SSFP vs. b-SSFP	13.7% vs. 9.8%	0.687
	T2W b-SSFP vs. SSFSE	13.7% vs. 7.8%	0.508
	b-SSFP vs. SSFSE	9.8% vs. 7.8%	1.000

APB abnormal placental bulge, *DIB* dark intraplacental bands, *PH* placental heterogeneity, *PPAS* placental protrusion into adjacent structures

In normal placentation, extravillous trophoblast invades the decidua and converts the spiral arterioles of the endometrium to uteroplacental vessels (decidualisation); the trophoblastic proliferation leads to the formation of chorionic villi. If the underlying endometrium is deficient, decidualisation fails and the chorionic villi invade and penetrate the myometrium. Prior caesarean section and placenta praevia are the two most important risk factors for PAD. Other proposed risk factors include conservative myomectomy, uterine artery embolization, curettage and previous uterine rupture [18]. Our study cohort also had high rates of placenta praevia (78.4%) and histories of caesarean delivery (82.3%), myomectomy (17.6%) and curettage (17.6%).

The diagnosis of PAD by MRI was first reported in the radiology literature in 1997 [19], with an increasing number of relevant studies published since then [15]. Compared with ultrasound, MRI is now considered significantly better in assessing depth of placental invasion, accurately reclassifying the extent of invasive placentation in up to 30% of patients and detecting signs of invasive placentation earlier [8, 20].

Because pregnant patients may have difficulty remaining supine, maintaining breath hold or lying still for extended periods of time, a fast free-breathing sequence should be prioritized; the most used are b-SSFP and SSFSE. SSFSE is valuable for evaluation of the uterine layers, placental architecture, foetal anatomy and adjacent organs [1, 13]. B-SSFP is widely used in foetal imaging, with the advantages of rapid scanning, freezing of foetal motion, high SNR for very short TR and without the point-spread-function blurring of SSFSE [21, 22].

In b-SSFP, the flip angle has a key role in the image contrast. When the flip angle is small, the image contrast is controlled by T1, and when the turning angle increases, the T2 component increases (like T2/T1). When the flip angle reaches 180°, image contrast is controlled by T2. At a flip angle of 180°, b-SSFP is similar to FSE: both sequences start with a 90° excitation pulse and then a series of 180° refocusing pulses [11, 23]. For b-SSFP, when the TE was set to equal to TR/2, the field inhomogeneity-induced dephasing is nearly completely refocused, which leads to the absence of T*2 effects, and therefore no signal dropout [24]. Therefore, the T2W b-SSFP and b-SSFP sequences were set to TE = TR/2. B-SSFP is sensitive to field inhomogeneities, which leads to banding artefacts. Short TR, volume shimming and maximum bandwidth were used to minimise such inhomogeneities and artefacts [11, 21]. In the preliminary experiment before the start of this study, we found that the minimum bandwidth

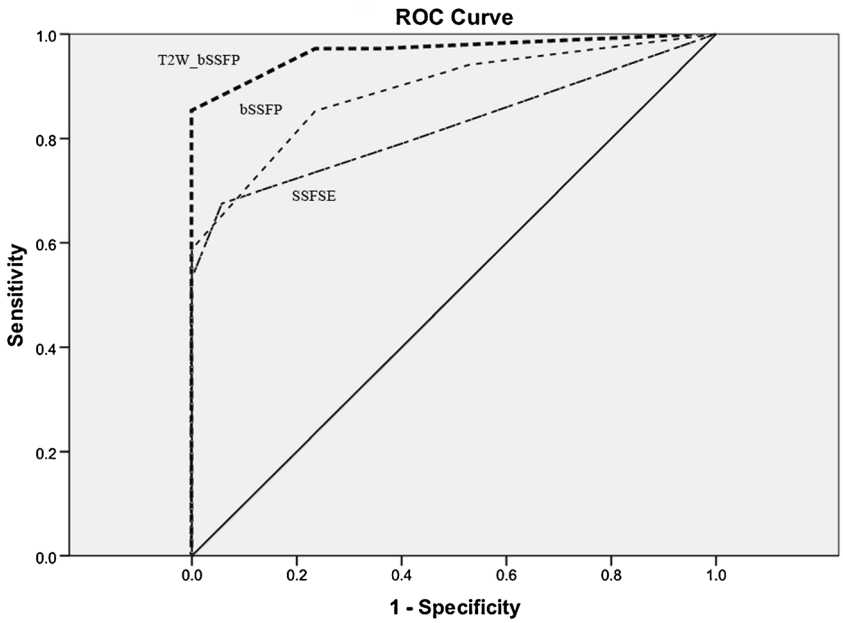

Fig. 6 ROC curves for diagnostic accuracy of PAD. The AUCs were 0.966, 0.890 and 0.823 for T2W b-SSFP, b-SSFP and SSFSE, respectively. $p < 0.001$ for each

(maximum water–fat shift) led to long TR, high SNR and more artefacts. The maximum bandwidth (minimum water–fat shift) led to short TR, low SNR and fewer artefacts. To obtain a balance between high SNR and low banding artefacts, the TRs of T2W b-SSFP and b-SSFP were set to 5 ms, and the water–fat shift was set in the range of 0.42 to 0.58 to maintain the TE = TR/2.

The signal ratio of the myometrium-to-placenta was found higher in T2W b-SSFP than in b-SSFP, which can be explained by the heavily T2W characteristic of the former. Yet the higher ratio in T2W b-SSFP compared with SSFSE may be due to the vascular proliferation and dilation in maternal myometrium during gestation [25], and vessels show a high signal in the SSFP sequence due to signal-enhancing inflow effects [11, 24].

There are five common diagnostic of PAD in MRI: abnormal uterine bulge, DIB, abnormal intraplacental vascularity, PH and PPAS [15]. Abnormal uterine bulge appears as a widening of the lower uterine segment, giving the uterus an hourglass-like configuration on coronal or sagittal images [26]. However, as a result of uterine wall thinning at late pregnancy, the boundary of the wall of the uterus is difficult to judge. The bulge is largely due to the placenta and not the uterine wall in this situation. In some cases, a thickened uterine wall is due to congestion and dilatation of the vessels, and the placental bulge does not necessarily result in the bulging of the uterine contour. Therefore we use the term "abnormal placenta bulge" rather than "abnormal uterine bulge" in this study.

T2 dark bands most often originate from the basilar plate at the maternal side of the placenta, with a length greater than 2 cm, and show a lower signal on b-SSFP images, in contrast to vascular lacunae, which appear hyperintense. This sign corresponds to areas of fibrin deposition observed on histopathology and is a sequelae of haemorrhage [14].

Abnormal intraplacental vascularity has been defined as flow voids at least 6 mm in diameter on T2 SSFSE sequences, with corresponding hyperintensity on b-SSFP sequences. Histopathologically, these appear as dilated placental vascularity [4]. Since the present study read b-SSFP and SSFSE images separately, this sign was not included.

The rate of PH increases with gestational age [27]. Areas of placental infarct may also contribute to a heterogeneous appearance. Slight PH is not significantly associated with placenta accreta, although marked heterogeneity in the placental signal due to haemorrhage or vascularity is putatively an indicator of PAD [14, 27]. To avoid repetition, if the placental signal is essentially homogeneous except for the sign of a T2 dark band, this situation should not be considered PH.

PPAS means extension of the placental tissue beyond the uterine serosa into the parametrium or bladder, or protrusion into the internal cervical os. This is a diagnostic sign of placenta percreta, and is more readily observed on MRI than sonography [15].

Table 4 The diagnostic sensitivity, specificity and Youden index of three signs in T2W-bSSFP (APB, DIB and PH) for accreta vera and increta

Sign	Sensitivity	Specificity	Youden index
APB	92.6%	76.5%	69.1%
DIB	77.8%	88.2%	66%
PH	66.7%	76.5%	43.2%

In the present study, the detection rate of APB was higher in the T2W b-SSFP and b-SSFP than in the SSFSE. This can be explained, firstly, because T2W b-SSFP and b-SSFP have higher signal contrast between the myometrium and placenta. Secondly, T2W b-SSFP and b-SSFP offer higher SNR than SSFSE does. Because a partial Fourier technique is used in SSFSE, only slightly more than half of the k space is filled, which leads to a reduced SNR [22, 28]. Thirdly, T2W b-SSFP and b-SSFP do not have the blurring effect that is seen in SSFSE. Because the single-shot technique uses significantly longer echo trains, there is more T2 decay during the acquisition time than with fast spin echo. This T2 decay causes signal variation between successive echoes, resulting in image blurring [22, 28].

In the present study, the detection rate of DIB was higher in the T2W b-SSFP than in the SSFSE. This may be related to the inherent sensitivity of b-SSFP to off-resonance signal changes caused by paramagnetic haemorrhage or its sequelae, although possessing spin-echo-like properties [29, 30]. The rate of PH was highest in the T2W b-SSFP images, probably because T2W b-SSFP is more sensitive to the off-resonance signal changes caused by haemorrhage or infarction and high signal of vessels in T2W b-SSFP also increase the heterogeneity of placenta. PPAS is more obvious on all three MRI sequences compared with less severe signs of PAD, and in the present study all the sequences were comparable for rates of detection.

In terms of the diagnostic accuracy of PAD, the maximum AUC was obtained from the T2W b-SSFP images. This may be related to the aforementioned high SNR, lack of blurring, and sensitivity off-resonance signal changes. For placenta accreta vera and increta, we found that the most sensitive and specific sign appearing on T2W_bSSFP was APB and DIB respectively, and the Youden index of PH was the lowest one. This may indicate that the APB and DIB appearing on T2W_bSSFP were better signs for diagnosing placenta accrete vera and increta. In a systematic review of MRI features of PAD, the most frequently encountered in cases of PAD were abnormal uterine bulging, heterogeneous placenta and T2 dark intraplacental bands, with the last being the most sensitive measure [31]. As pregnancy progresses, PH may be a normal finding, especially in the third trimester [27]. The gestational age at acquisition in this study is also in third trimester (greater than 28 weeks), which may also have caused more PH. T2W b-SSFP is relatively sensitive to displaying PH, and this may undermine its diagnostic value.

Conclusion

Our results indicate that T2W b-SSFP has a relatively high diagnostic accuracy for PAD, which may be due to its high SNR, T2-weighting, clear images with no blurring, and sensitivity to off-resonance signal changes.

Funding The authors state that this work has not received any funding.

Compliance with ethical standards

Guarantor The scientific guarantor of this publication is Ang Yang.

Conflict of interest The authors of this manuscript declare no relationships with any companies whose products or services may be related to the subject matter of the article.

Statistics and biometry No complex statistical methods were necessary for this paper.

Informed consent Written informed consent was obtained from all subjects in this study.

Ethical approval Institutional review board approval was obtained.

Methodology
- prospective
- diagnostic study
- performed at one institution

References

1. Baughman WC, Corteville JE, Shah RR (2008) Placenta accreta: spectrum of US and MR imaging findings. Radiographics (28): 1905–1916
2. Wu S, Kocherginsky M, Hibbard JU (2005) Abnormal placentation: twenty-year analysis. Am J Obstet Gynecol 192:1458–1461
3. Silver RM, Landon MB, Rouse DJ et al (2006) Maternal morbidity associated with multiple repeat cesarean deliveries. Obstet Gynecol 107:1226–1232
4. Ueno Y, Kitajima K, Kawakami F et al (2014) Novel MRI finding for diagnosis of invasive placenta praevia: evaluation of findings for 65 patients using clinical and histopathological correlations. Eur Radiol 24:881–888
5. Chantraine F, Blacher S, Berndt S et al (2012) Abnormal vascular architecture at the placental-maternal interface in placenta increta. Am J Obstet Gynecol 207:188.e1–188.e9
6. Eshkoli T, Weintraub AY, Sergienko R, Sheiner E (2013) Placenta accreta: risk factors, perinatal outcomes, and consequences for subsequent births. Am J Obstet Gynecol 208:219.e1–219.e7
7. Committee on Obstetric Practice (2012) Committee opinion no. 529: placenta accreta. Obstet Gynecol 120:207–211
8. Lim PS, Greenberg M, Edelson MI et al (2011) Utility of ultrasound and MRI in prenatal diagnosis of placenta accreta: a pilot study. AJR Am J Roentgenol 197:1506–1513
9. Derman AY, Nikac V, Haberman S et al (2011) MRI of placenta accreta: a new imaging perspective. AJR Am J Roentgenol 197: 1514–1521
10. Masselli G, Brunelli R, Parasassi T et al (2011) Magnetic resonance imaging of clinically stable late pregnancy bleeding: beyond ultrasound. Eur Radiol 21:1841–1849
11. Scheffler K, Lehnhardt S (2003) Principles and applications of b-SSFP techniques. Eur Radiol 13:2409–2418
12. Hood MN, Ho VB, Smirniotopoulos JG et al (1999) Chemical shift: the artifact and clinical tool revisited. Radiographics 19:357–371

13. Levine D, Hatabu H, Gaa J, Atkinson MW, Edelman RR (1996) Foetal anatomy revealed with fast MR sequences. AJR Am J Roentgenol 167:905–908
14. Lax A, Prince MR, Mennitt KW et al (2007) The value of specific MRI features in the evaluation of suspected placental invasion. Magn Reson Imaging 25:87–93
15. D'Antonio F, Iacovella C, Palacios-Jaraquemada J et al (2014) Prenatal identification of invasive placentation using magnetic resonance imaging: systematic review and meta-analysis. Ultrasound Obstet Gynecol 44:8–16
16. Oyelese Y, Smulian JC (2006) Placenta previa, placenta accreta, and vasa previa. Obstet Gynecol 107:927–941
17. Sentilhes L, Gromez A, Clavier E et al (2011) Long-term psychological impact of severe postpartum hemorrhage: hemorrhage and psychological issues. Acta Obstet Gynecol Scand 90:615–620
18. Josephs SC (2008) Obstetric and gynecologic emergencies: a review of indications and interventional techniques. Semin Intervent Radiol 25:337–346
19. Levine D, Hulka CA, Ludmir J et al (1997) Placenta accreta: evaluation with color Doppler US, power Doppler US, and MR imaging. Radiology 205:773–776
20. Masselli G, Brunelli R, Casciani E et al (2008) Magnetic resonance imaging in the evaluation of placental adhesive disorders: correlation with color Doppler ultrasound. Eur Radiol 18:1292–1299
21. Haacke EM, Wielopolski PA, Tkach JA et al (1990) Steady-state free precession imaging in the presence of motion: application for improved visualization of the cerebrospinal fluid. Radiology 175: 545–552
22. Chung HW, Chen CY, Zimmerman RA et al (2000) T2 weighted fast MR imaging with true FISP versus HASTE: comparative efficacy in the evaluation of normal foetal brain maturation. AJR Am J Roentgenol 175:137580
23. Zur Y, Stokar S, Bendel P (1988) An analysis of fast imaging sequences with steady-state transverse magnetization refocusing. Magn Reson Med 6:17–193
24. Scheffler K, Hennig J (2003) Is TrueFISP a spin-echo or gradient-echo sequence? Magn Reson Med 49:395–397
25. Lunell NO Nylund L (1992), Uteroplacental blood flow. Clin Obstet Gynecol 35:108
26. Leyendecker JR, DuBose M, Hosseinzadeh K et al (2012) MRI of pregnancy-related issues: abnormal placentation. AJR Am J Roentgenol 198:311–320
27. Blaicher W, Brugger PC, Mittermayer C et al (2006) Magnetic resonance imaging of the normal placenta. Eur J Radiol 57:256–260
28. Mittal TK, SFS H, Bourne MW et al (1999) A prospective comparison of brain contrast characteristics and lesion detection using single-shot fast spin-echo and fast spin-echo. Neuroradiology 41: 480–486
29. Scheffler K, Seifritz E, Bilecen D et al (2001) Detection of BOLD changes by means of a frequency sensitive trueFISP technique: preliminary results. NMR Biomed 14:490–496
30. Scheffler K, Hennig J (2003) Is TrueFISP a gradient-echo or a spin-echo sequence? Magn Reson Med 49:395–397
31. Rahaim NSA, Whitby EH (2015) The MRI features of placental adhesion disorder and their diagnostic significance: systematic review. Clin Radiol 70:917–925